Automatic Rigid Registration of Aortic Aneurysm Arterial System

Gwladys Ravon, Florian Bernard, Angelo Iollo, Caroline Caradu

Automatic Rigid Registration of Aortic Aneurysm Arterial System

Gwladys Ravon*[1], Florian Bernard[2], Angelo Iollo[1,3], and Caroline Caradu[4]

[1]Inria - Bordeaux Sud-Ouest, Team MEMPHIS, 33405 Talence, France
[2]Nurea, 33000 Bordeaux, France
[3]IMB, UMR 5251, Université de Bordeaux, 33405 Talence, France
[4]Groupe hospitalier Pellegrin, Unit of Vascular Surgery, CHU Bordeaux, 33000 Bordeaux, France

Abstract

An abdominal aortic aneurysm is defined as a local and abnormal dilation of the aortic wall that can lead to rupture and death without treatment. A useful tool for the patient's postoperative follow-up is segmentation registration to see the evolution of the aneurysm between two examinations. Here, we propose a method to automatically register the entire arterial system: the segmentation is divided in three parts (suprarenal, infrarenal zone, and iliac arteries) and each part is registered separately. We chose a rigid point set to point set registration through the iterative closest point algorithm. We also compute the displacement fields and derive a criterion to accept or reject the registration of the infrarenal zone and iliac arteries. Registration is successful in 96% of cases for the infrarenal zone, in 94% for the suprarenal zone and in 65% for the iliac arteries.

1 Introduction

An abdominal aortic aneurysm is defined as a local and abnormal dilation of the aortic wall. Without treatment the aneurysm may grow until rupture, which ultimately leads to death in a majority of cases [5, 8]. The preferred treatment modality now consists in the implantation of an endograft inside the aorta inserted through a sheath through the femoral arteries (endovascular aortic aneurysm repair (EVAR) [4]). The endograft isolates the aneurysm wall from the blood flow. Although it is a less invasive and morbid procedure procedure, the need for post-operative surveillance on a

*Corresponding author: gwladys.ravon@inria.fr

long time scale is important [11]. The registration of information (images, centerlines or segmentations) obtained at different time points after the procedure is an important tool to follow the evolution of the aneurysm. It allows the clinician to see whether the aneurysm has grown or shrunk and where. Different approaches have been developed in the past years and we can cite the studies from Maiora et al. [10], Lopez-Linares et al. [9], Braet et al. [2] or Demirci et al. [6]. These works have in common to combine several steps: they start with a rigid registration and the final step consists of a non-rigid deformation to align both objects and deduce the displacement field of the aneurysm between the two examinations. Another common point among these approaches is that at least one step of the process relies on the intensity of the images, thus the methods are not suitable for cases with no contrast agent. On the other hand, the basis for the rigid registration differ from one study to another: bones (Lopez-Linares et al.), lumen (Maiora et al.) or images (Braet et al. and Demirci et al.). The basis for the non rigid registration is also different: thrombus (Lopez-Linares et al.), lumen (Maiora et al.), images (Braet et al.) or centerlines (Demirci et al.). Methods are visually validated by experts, but a metric can be used to follow the improvement of the result at each step of the process. These four studies focus on the aneurysm in the infrarenal zone and neglect the suprarenal zone and the iliac arteries.

In the present work, we propose a new method to register the arterial system based on a rigid point set registration. We chose a rigid transformation because we wanted to keep the aneurysm unchanged. Because of the patient's movement and breathing, the relative position of the arterial system may be different for different examinations, especially the outer parts. For this reason, in the following, segmentations were automatically divided into three parts (suprarenal, infrarenal zone and iliac arteries) and each part was registered independently. Cutting the segmentations was also useful to deal with different topologies: presence or absence of the aortic root, length of the iliac arteries, etc. Assuming a displacement in the normal direction we computed displacement fields and derived a criterion to accept or reject a registration without a visual validation.

2 Methods

2.1 Registration

Registration was performed based on an initial random distribution of points on the aortic wall (the outer surface of the segmentation) using the Iterative Closest Point (ICP) algorithm first introduced by Besl and McKay [1]. The method finds the transformation between two points clouds by minimizing the lowest distances between points (root mean square error). In the following, the number of points on each surface was set to 200. To improve the

possibility of finding a global minimum we started by matching the centroids of the segmentations. In synthesis, by combing ICP and centroid matching, we determine an optimal rigid roto-translation that keeps the shape of the aneurysm unaltered.

Our objective is to study segmentations that are the result of an automatic workflow. Hence, as function of the image and the conditions of the scan setting, the data can correspond to different portions of the vascular network containing the aneurysm. Therefore, we initially performed the registration of the full segmentation which could go, for instance, from the lowest extremities to the aortic arch. However, the results were not satisfying since the ICP algorithm could not converge to a meaningful minimum if the branches of the two segmentations were too different. As a result, the registration of the full segmentation could not lead to an overall acceptable result.

The key point is to divide the segmentation into comparable regions. In this case, three parts: the suprarenal and infrarenal zones and the iliac arteries. Then, they were registered separately. As we wanted the workflow to be automatic, we developed our own cutting method (Riffaud et al, submitted). This method identifies the different branches of the arterial system from the abdominal aortic aneurysm segmentation, through the centerline and its bifurcation points. The application of this method to our segmentation identified the bifurcations of the renal arteries and the aortic bifurcation. Once the vascular branches are correctly identified, the segmentation is cut above the highest renal artery and 30 mm below the aortic bifurcation. Retention of the renal and incipient iliac arteries was suitable to ensure the finding of the correct rotation.

Additional preprocessing was required for the three regions. First, we needed to remove outliers from the renal arteries for the infrarenal zone. Regarding the suprarenal zone, both the celiac artery and the superior mesenteric arteries led the ICP algorithm to a local minimum rather than the global minimum. It was even less effective in presence of complex curved vessels. We had to remove them to ensure a good result. To this end, we applied an erode filter to both segmentations. To avoid problems caused by the presence of the aortic arch in only one segmentation, we kept the same height of the aorta for the target and the source. It was determined as the smallest height between the 2 suprarenal zones. We performed the registration of the two corresponding surfaces and applied the transformed matrix to the original source surface.

Regarding the iliac arteries, we registered separately the right and left common iliac arteries to minimize the impact of patient's motion. To ensure convergence to a global minimum we kept the same length on both segmen-

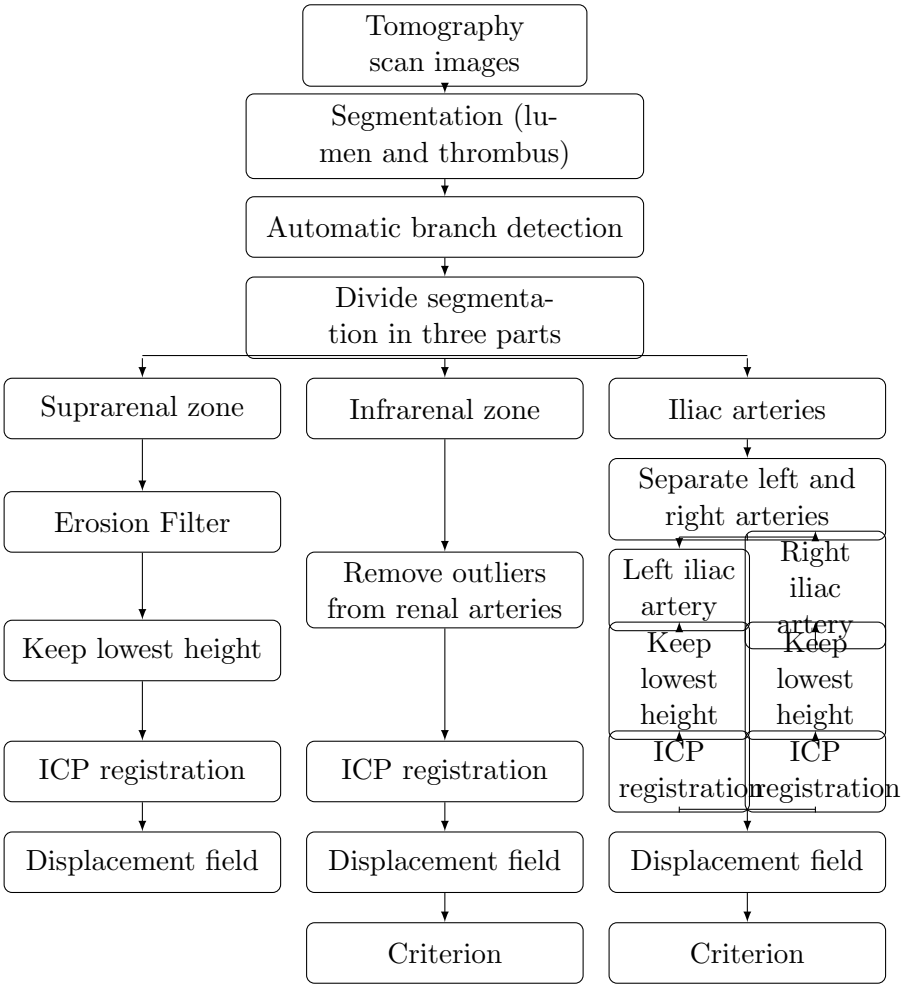

Figure 1: Schematic representation of the automatic registration pipeline

tations. A schematic representation of entire the workflow can be founded in Figure 1.

2.2 Displacement fields

We computed the displacement fields in the normal direction of the aneurysm between two scans. For each point on the target surface, we determined if it was inside (respectively outside) the registered source surface. We then found the closest intersection point with the registered source in the outward (resp. inward) normal direction, at most at 20 millimeters. The positive (resp. negative) euclidean distance between the two points determined the value of the displacement. An example can be seen in Figure 2: we represented displacement fields from dark blue if the aneurysm had significantly

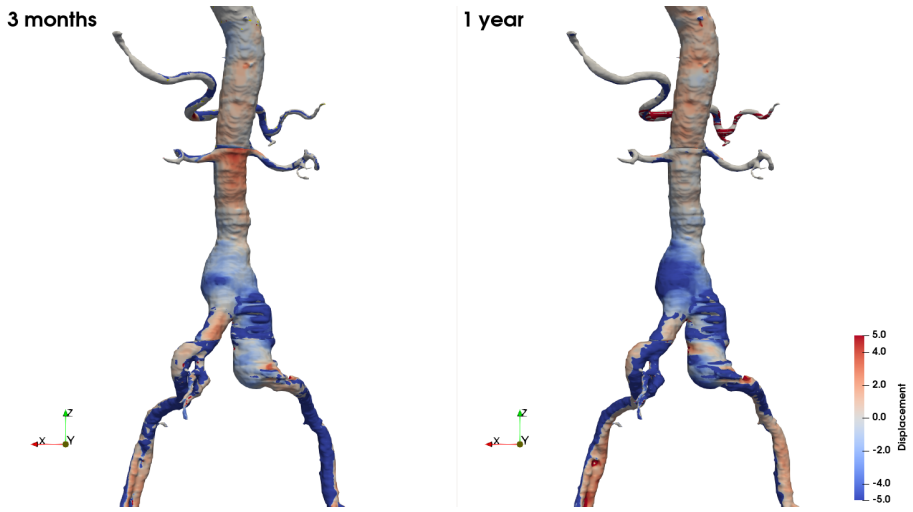

Figure 2: Displacement fields for Patient A 3 months and 1 year after the procedure. The target surface was the one from the post-operative scan

shrunk to dark red if it had grown. Light blue and red stand for small values of the displacement field. The shrinking of the aneurysm for Patient A is visible at 3 months post-EVAR and was more important 1 year after the procedure, even in the right common iliac artery.

2.3 Accepted and rejected registrations

All the registrations were visually evaluated by experts and registration was rejected when one could notice a left-right or top-bottom shift, or when it was visible that the rotation was wrong. In the figures white surfaces are the target surfaces, obtained from the first post-EVAR examination. Red surfaces are the registered source surfaces from the second examination. Figure 3 shows examples of rejected registrations of the full geometry: for Patients A and C there were lateral shifts, whereas for Patient B it was a vertical shift. We show examples of accepted registrations of the infrarenal zone for the three same patients in Figure 4.
Figure 5 exhibits rejected registrations of suprarenal zones for the same patients: mainly the rotation was not good. Figure 6 shows accepted registration of the same patients with our proposed method. Concerning the iliac arteries Figure 7 shows accepted registrations for Patient A and B even though the end of the iliac arteries did not match well. This was expected due to the changes in the patient's position. For Patient C, the registration was rejected because of a slight sub-shift.

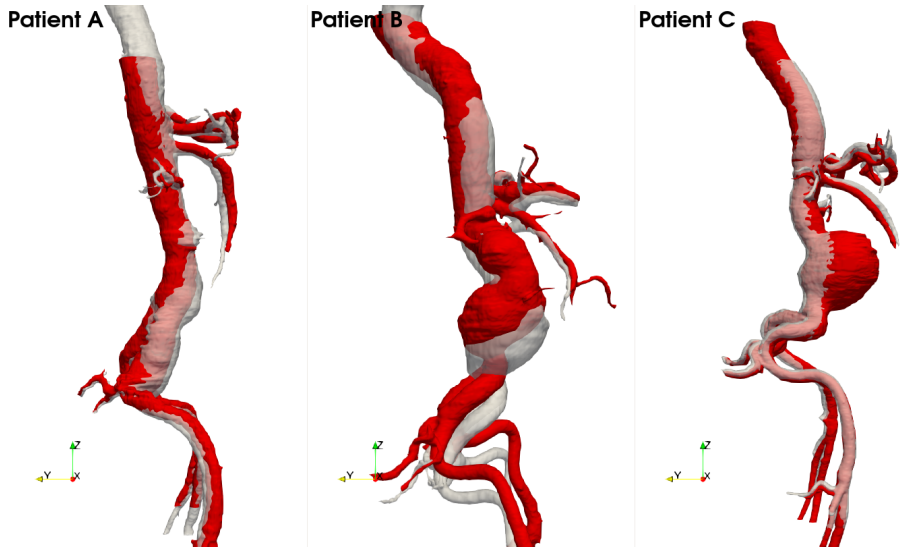

Figure 3: Example of registration of the full surface for 3 patients. White surfaces are the target surfaces, obtained from the first post-EVAR examination. Red surfaces are the registered source surfaces from the second examination

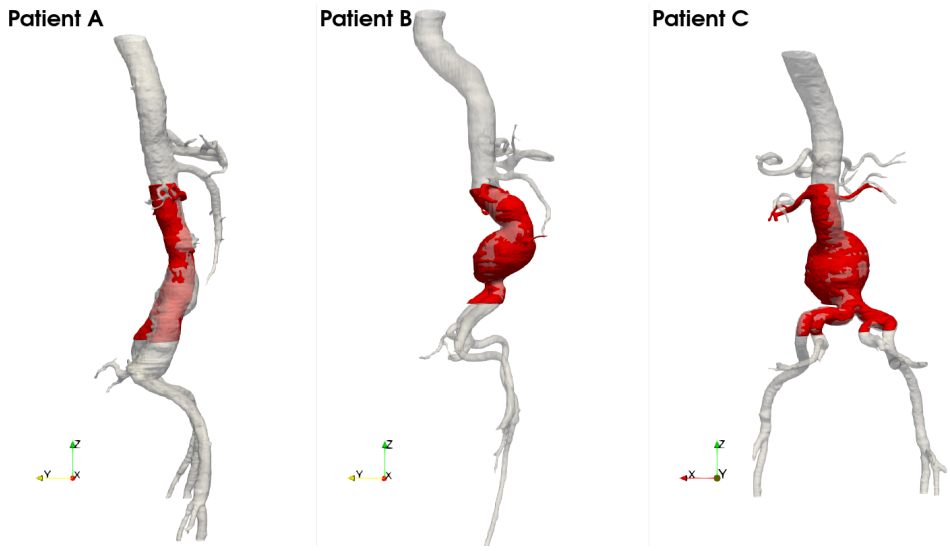

Figure 4: Registration of the infrarenal zone for Patients A, B and C. Registered infrarenal zone is superimposed on the full geometry

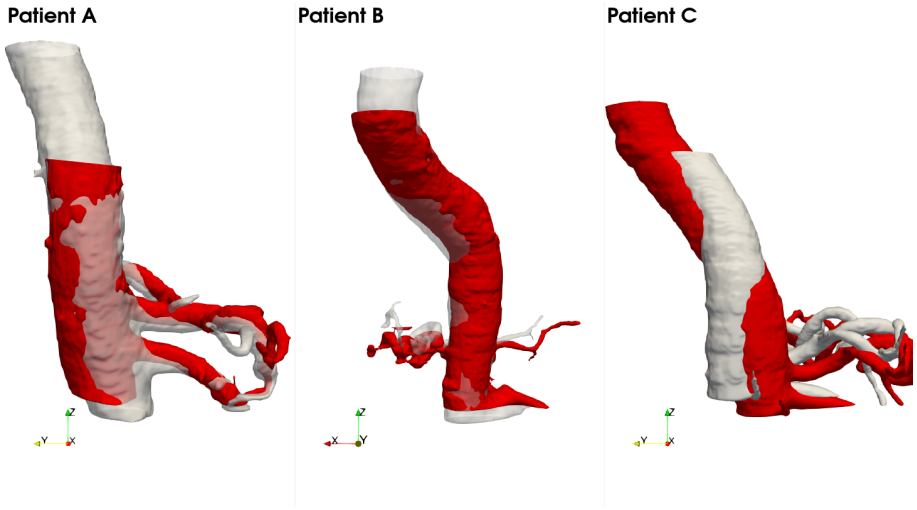

Figure 5: Regular ICP of the suprarenal zone for Patients A, B and C

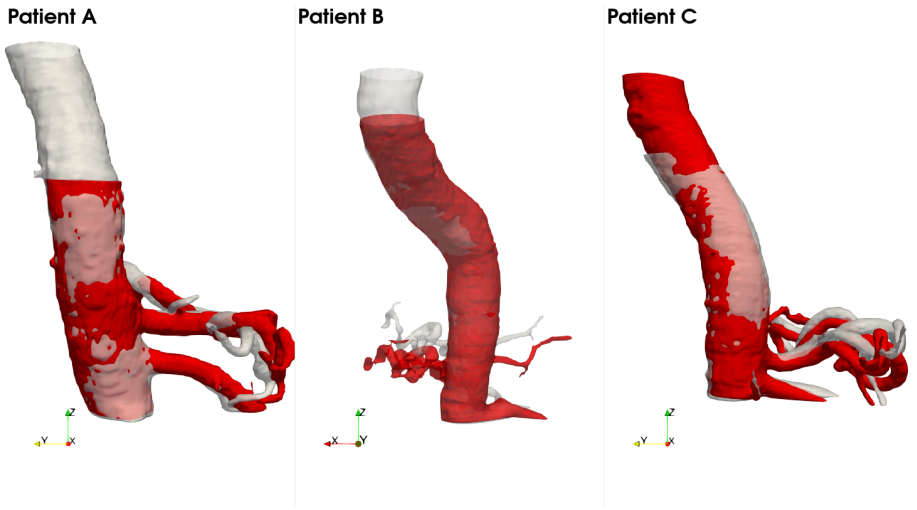

Figure 6: Registration of the suprarenal zone for Patients A, B and C after pre-processing

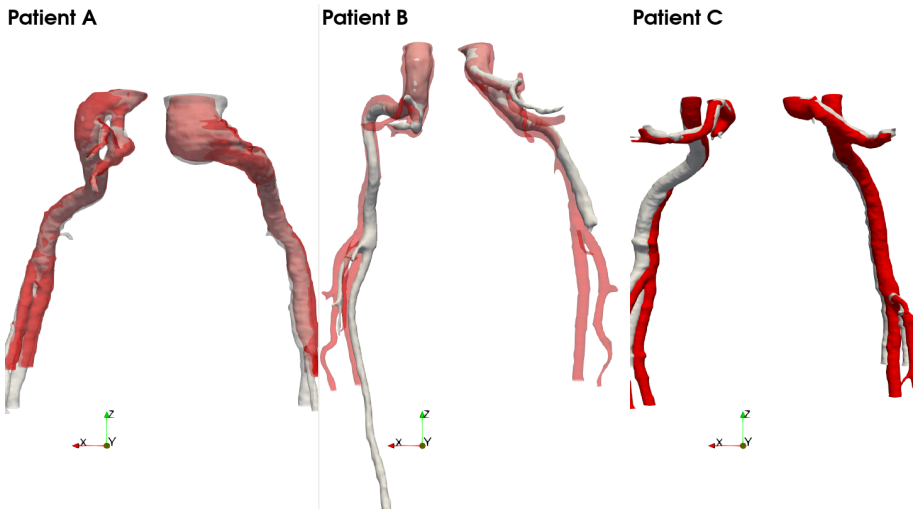

Figure 7: Registration of the iliac arteries for Patients A, B and C

2.4 Criterion

With the goal of automatically distinguishing an accepted registration from a rejected one, we searched for a criterion based on the statistics of the values of the displacement field.

To evaluate the registration of the full geometry and the infrarenal zone we automatically select a centered 10-millimeter-thick slab at the point with the largest axial diameter (see Figure 8). For the suprarenal zone, we considered the lowest 30 millimeters of the segmentation and the 30 highest for the iliac arteries.

We then computed the median (M) and the first (Q_1) and third (Q_3) quartiles of the displacement field values on these slabs. We introduce the product

$$\mathcal{P} = Q_1 * Q_3. \tag{1}$$

This product $\mathcal{P}$ indicates if there is a change in the sign of the displacement field, which could correspond to a shift in the registration. On the other hand, if the product is positive it means that the aneurysm has evolved in the same way on the full slab: either shrunk or grown. We also define the dispersion $\mathcal{D}$ as

$$\mathcal{D} = Q_3 - M. \tag{2}$$

This quantity gives an indication of the dispersion of the displacement field values. In the next section, the objective is to find a threshold value for $\mathcal{D}$ to accept or reject a registration, depending on the sign of $\mathcal{P}$.

Figure 8: Example of a slab around the point with the highest axial diameter. Segmentation (blue), centerline colored with the diameter values and 10 millimeters thick slab

2.5 Dataset

The dataset was composed of segmentations from 42 different patients for a total of 81 registrations with always the segmentation obtained right after the procedure as the target segmentation. All the segmentations were provided by Nurea (`https://www.nurea-soft.com`). The methodology was validated by clinicians and was the object of the study published by Caradu et al. [3].

3 Results

All the registrations were visually labeled as accepted or rejected by experts.

3.1 Full geometry and infrarenal zone

Among the 81 registrations of the full geometries, only 11 were accepted. Among the 70 rejected 36 were of really poor quality with no superposition of the target and the registered source (see Figure 9 for an instance). Most of the time this was due to an important difference in the topology like the presence or absence of the aortic arch. When we computed the displacement fields, it was initialized to zero, so if the registered source was too far from

Figure 9: Example of rejected and very poor registration of full segmentations

the target, it remained null. That led the product $\mathcal{P}$ to be null as well: it is a rejection criterion.
Regarding the registrations of the infrarenal zones, 78 were accepted (96%) and none were of really poor quality. There was a problem with the segmentation in the 3 rejected cases: artifacts or superior mesenteric artery glued to the sac.
Figure 10 shows the distribution of $\mathcal{D}$ depending on the sign of $\mathcal{P}$ for rejected and accepted registrations. One can see that a threshold can be found to distinguish rejected registrations from accepted ones, especially when the product $\mathcal{P}$ is negative. To find those thresholds we used a Support Vector Machine (SVM) algorithm with a linear kernel on two sets: positive product on one hand, negative product on the other hand. We then predicted the output (accepted or rejected) for a range of dispersion values between 0.1 and 10 with a step of 0.1. The results can be seen in Figure 11: the threshold for a negative product was much smaller than for a positive product, respectively 1.6 and 3.54. If we applied these thresholds on our registrations, 11 would have been wrongly accepted (10 full geometries and 1 infrarenal zone) and 2 would have been wrongly rejected (2 infrarenal zone).

In short, a registration should be rejected in the following cases:

- $\mathcal{P} = 0$,
- $\mathcal{P} < 0$ and $\mathcal{D} > 1.6$,

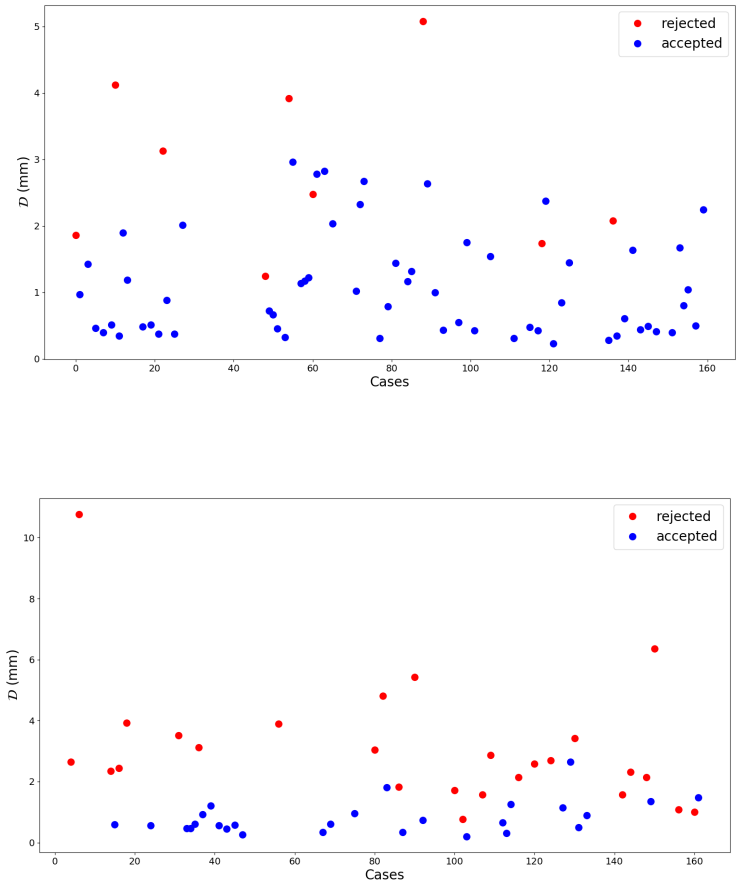

Figure 10: Dispersion $\mathcal{D}$ for registrations of the full geometries and the infrarenal zones. Top: $\mathcal{P} > 0$, bottom: $\mathcal{P} < 0$. Red: rejected registrations; blue: accepted ones

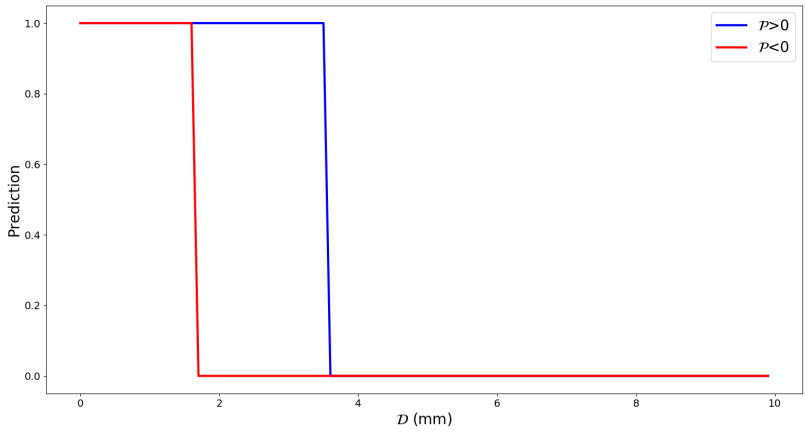

Figure 11: Predictions from SVM algorithm for a range a dispersion values between 0.1 and 10. Red line: $\mathcal{P} < 0$, blue line: $\mathcal{P} > 0$

- $\mathcal{P} > 0$ and $\mathcal{D} > 3.54$.

3.2 Suprarenal zone

For the suprarenal zone, only 5 registrations were rejected including 3 with artifacts and 2 with a thin aorta. Only 3 cases had a positive product $\mathcal{P}$ so we did not make any distinction according to its sign. In Figure 12 we can see that no distinction can be made between values for accepted and rejected registrations. When we applied an SVM algorithm, the threshold between accepted and rejected was 86 in the linear case and 135 in the non-linear case which was not relevant. Moreover, when we removed the isolated accepted case, the predictions always resulted in "accepted" in both cases, which may be due to the small number of rejected cases. We can assume that the registration is accepted if the segmentations are correct.

3.3 Iliac arteries

Registration of this part was the most difficult because of the shape of the iliac arteries: 53 registrations were accepted (65%). 20 were rejected with only one common artery correctly registered and 8 were rejected with both arteries badly registered. Among those 28 cases, 7 presented artifacts in the segmentation or had at least one very short common iliac artery. The success rate rises to 72% when the segmentations are clean. Only 6 cases had a positive product so it was meaningless to make a difference. The SVM algorithm on the distribution of the dispersion $\mathcal{D}$ visible in Figure 13

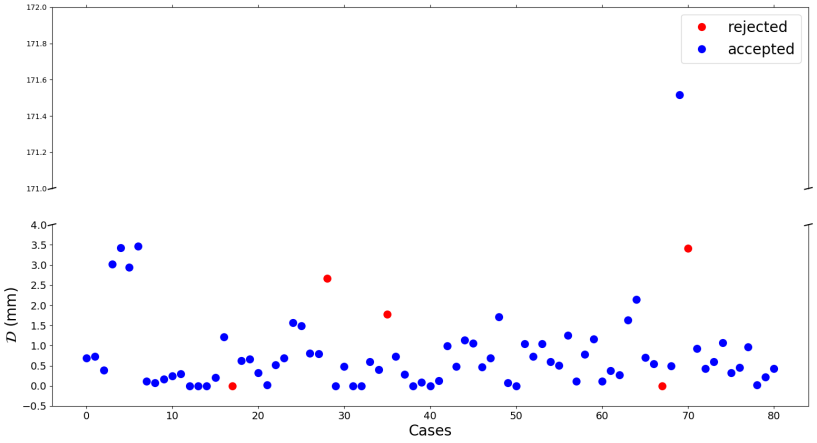

Figure 12: Dispersion $\mathcal{D}$ for registrations of the suprarenal zones

won't be relevant. However, a dispersion $\mathcal{D}$ greater than 7 mm indicates a non-satisfying registration. 9 cases had a null product $\mathcal{P}$, including 4 with artifacts or short iliac arteries. In short, a registration of the iliac arteries should be rejected in the following cases:

- $\mathcal{P} = 0$,
- $\mathcal{P} \neq 0$ and $\mathcal{D} > 7$.

13 registrations would have been rightly rejected while 4 would have been wrongly rejected. In 2 cases the source was cut lower than the target so that only a small portion of the registered source was within the 30 mm considered for the computation of the dispersion $\mathcal{D}$.

Figure 14 presents the results with the three different parts on the same image for Patients A, B and C. Small discontinuities can be seen between parts on Patients B and C.

3.4 Evolution in time: example of patients' follow-up

Follow-up of the surgery includes regular examinations to control the evolution of the aneurysm. That is why we had multiple segmentations for a given patient and could perform registration by parts of these segmentations. The target surface was always the surface from the scan performed immediately after the procedure. For Patient A we had two segmentations obtained after 3 months and 1 year. In Figure 15 one can see that the aneurysm started to shrink after 3 months and the reduction was more important after one year. The aneurysm was also partially located in the right common iliac artery,

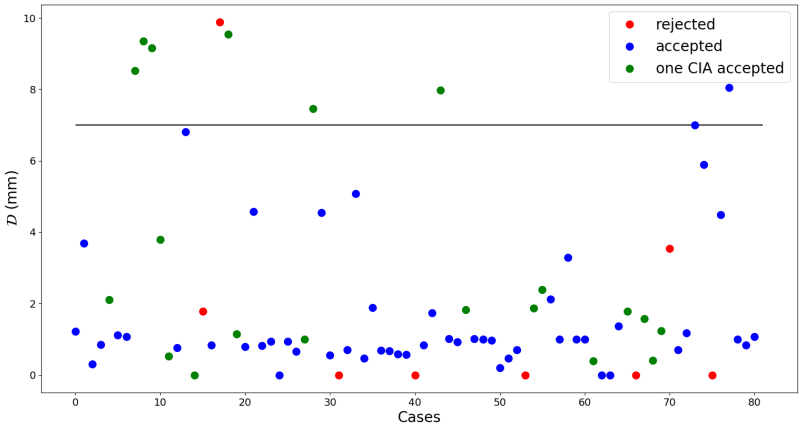

Figure 13: Dispersion $\mathcal{D}$ for registrations of the iliac arteries

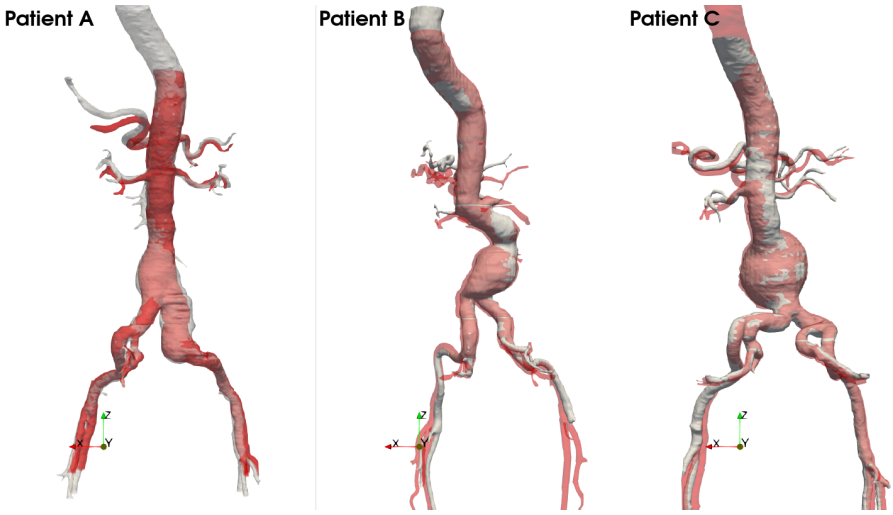

Figure 14: Registration of the three different parts for Patients A, B and C

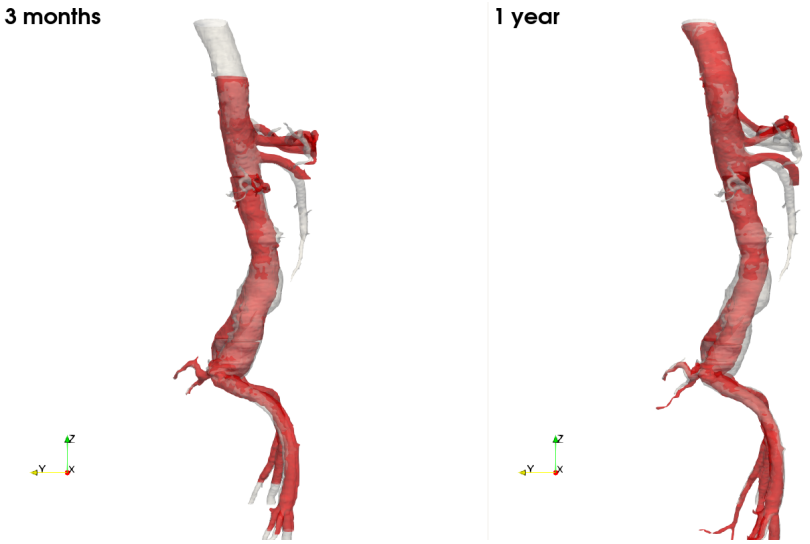

Figure 15: Registrations for Patient A 3 months and 1 year after the procedure. The target surface was the one from the post-operative scan

and this part had also shrunk. Displacement fields are displayed in Figure 2 from dark blue if the aneurysm had significantly shrunk to dark red if it had grown. Light blue and red stand for small values of the displacement field. Displacements were consistent with what we previously observed. The shrinking of the aneurysm for Patient A is visible at 3 months and was more important 1 year after the procedure, even in the right common iliac artery. For Patient B we had 4 scans: 3 and 6 months and 1 and 2 years after the procedure. Figure 16 shows that the aneurysm remained stable after 3 months. It then started to grow at 6 months, remained stable between 6 month and 1 year but then had a massive global growth after 2 years. With the displacement field (Figure17) we retrieved the stable-growth-stable-massive growth scheme.
For Patient C we had only one scan 4 months post-EVAR and the result is visible in Figure 14. The aneurysm seemed to be stable. However with the visualization of the displacement field (Figure 18) we can see that the aneurysm had grown. It shows that the aneurysm had grown locally on the back side of the sac while the front side remained stable. In this particular case, the maximum diameter had not changed despite an increasing volume.

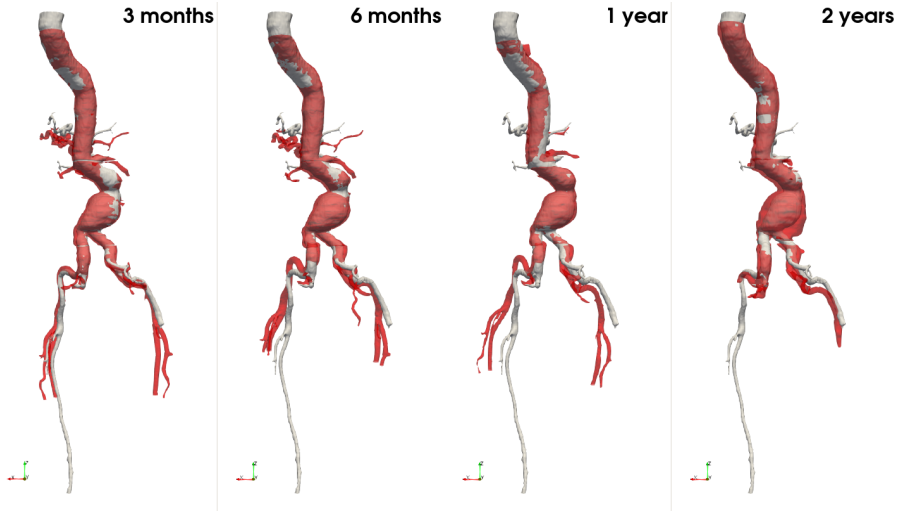

Figure 16: Registrations for Patient B for 4 scans after the procedure. The target surface was the one from the post-operative scan

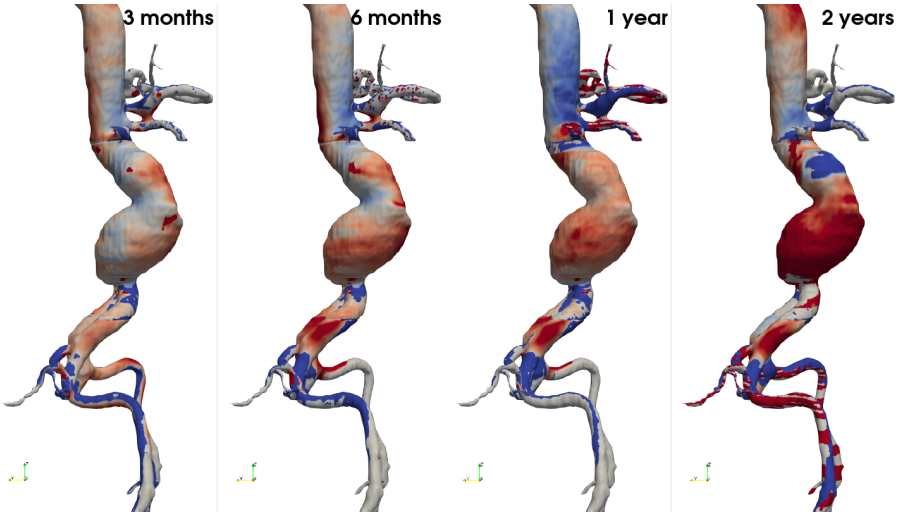

Figure 17: Displacement fields for Patient B for 4 scans after the procedure. The target surface was the one from the post-operative scan

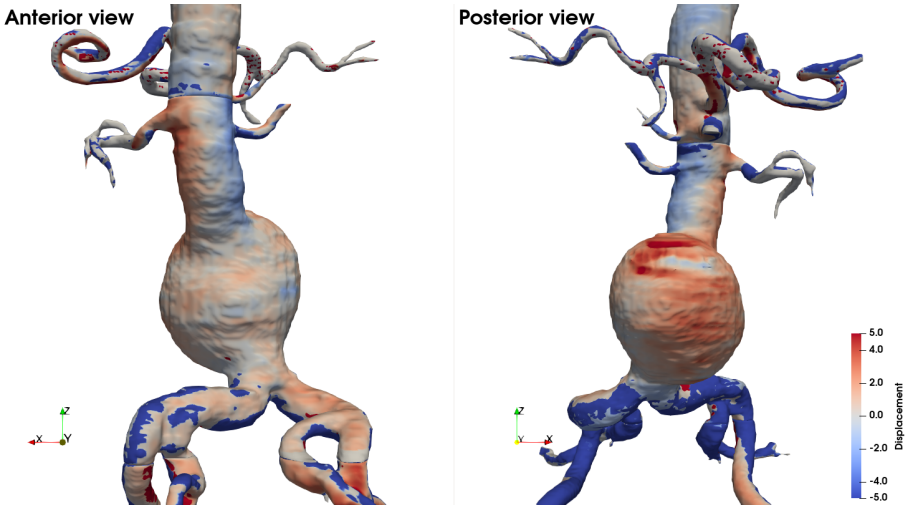

Figure 18: Different views of displacement fields for Patient C. The target segmentation was the one from the post-operative scan

4 Discussion and Conclusion

We have developed an automatic pipeline that registers the arterial system and allows visualization of an aortic aneurysm evolution for a patient between two examinations. Unlike other studies, we used a rigid registration and assumed that the aneurysm evolves in the normal direction to the wall of the aneurysm.

Registering the entire arterial system up to the iliac arteries, rather than just the aneurysm region, makes it possible to follow any aneurysm regardless of its location. We proposed a method based on the iterative closest point algorithm to register segmentations of abdominal aortic aneurysms. It registers not only the aneurysm region but the entire arterial system including the aorta and iliac arteries. Segmentations were divided into 3 parts: suprarenal, infrarenal zones and the iliac arteries. Each region was registered separately, after a preprocessing depending on the region. We have shown that registration of the infrarenal zone instead of the whole segmentation leads to better results in terms of expert assessment. Our method leads to accepted registrations in 96%, 94% and 65% of cases for the infrarenal and suprarenal zones and the iliac arteries, respectively. 78% of individual iliac arteries are registered in an acceptable manner.

Rigid registration allows an objective, model-free, comparison to evaluate the evolution of aneurysm surfaces. Clearly, the limitations of our approach are intrinsic to the minimization algorithm. In extreme situations, for example in the case of large variations in tortuosity, minimization will

somehow average the displacement of the centerline and that of the surfaces. We have also introduced the computation of displacement fields in the normal direction. The displacement field represents a quantitative indicator for the evaluation of the aneurysm's evolution. Its visualization is quite simple with the color scale. Based on its value, we have also developed a criterion to accept or reject the registration of the infrarenal part and the iliac arteries. None was required for the supra-renal zone. Our method, unlike other existing methods, is independent of the images or anatomic location of the aneurysm. It can be performed with or without contrast product and is not disturbed by the presence of artifacts in the image. It can also be interpreted as a preliminary step that can be used as a first step for non-rigid registration.

The choice of a point set registration algorithm was guided by the imperative of user-free usage. For example, a method that relies on landmark registration usually requires user intervention to select or validate landmarks which also involve uncertainty and inter-user variability. Moreover, the fewer landmark points considered, the more important the accuracy of the position of each point. In contrast, this problem is avoided with the aortic wall surfaces due to the systematic random sampling of the surfaces.

A known bias in aneurysm volume measurement is the cardiac cycle [12, 7]: it is not constant during the whole cycle. Part of the changes in volume or shape we observed could be attributable to a different phase of the cardiac cycle. However, this is impossible to quantify without having full control on the image acquisition. To avoid this bias, it would be necessary to register segmentations taken during the same phase. However, such information is not available from CT-scan images.

Registration is an important tool to follow the evolution in time of an aneurysm. As an example of application, we showed the results for 3 patients: one with a shrinking aneurysm (Patient A), one with a globally growing aneurysm (Patient B) and one with a locally growing aneurysm (Patient C). For Patient A, the aneurysm was also located in one common iliac artery. Thanks to our method we could follow its evolution and see that it had shrunk in the iliac artery too.

Author contribution

GR designed the study, implemented the algorithms, analyzed and interpreted the results and drafted the manuscript. FB and AI helped conceive the study, provided feedback about the results and revised the manuscript. CC provided expert analysis on the results and revised the manuscript.

Conflict of interest

The authors declare that they have no conflict of interest.

G. Ravon completed a PhD in applied mathematics at the University of Bordeaux. The subject mixed inverse problems and cardiac electrophysiology. She has currently a post-doctoral position at Inria Bordeaux Sud-Ouest in Memphis Team. Her main research topic is applied mathematics to medicine and health care.

F. Bernard completed a PhD in applied mathematics at University of Bordeaux and a PhD in fluid dynamics at Politecnico di Torino in 2015. He's now CEO of Nurea, a company dedicated to the development of decision making support software for physicians to improve diagnostic, follow up and pronostic of cardiovascular diseases.

A. Iollo is professor of Applied Mathematics at the University of Bordeaux and head of team Memphis at Inria, the national institute for applied mathematics and computer science.

Dr C. Caradu is a M.D. Ph.D. working as a vascular surgeon at the University Hospital of Bordeaux. Her research interests include the endovascular treatment of complex aortic aneurysms, the use of artificial intelligence in the treatment of vascular pathologies, aortic infections, and the role of endothelial cell dysfunction in the pathophysiology of critical limb ischemia.

References

[1] Besl, P.J., McKay, N.D.: Method for registration of 3-D shapes. In: P.S. Schenker (ed.) Sensor Fusion IV: Control Paradigms and Data Structures, vol. 1611, pp. 586 – 606. International Society for Optics and Photonics, SPIE (1992). DOI 10.1117/12.57955

[2] Braet, D.J., Eliason, J., Ahmed, Y., van Bakel, P.A., Zhong, J., Bian, Z., Figueroa, C.A., Burris, N.S.: Vascular deformation mapping of abdominal aortic aneurysm. Tomography **7**(2), 189–201 (2021)

[3] Caradu, C., Spampinato, B., Vrancianu, A.M., Bérard, X., Ducasse, E.: Fully automatic volume segmentation of infrarenal abdominal aortic aneurysm computed tomography images with deep learning approaches versus physician controlled manual segmentation. Journal of Vascular Surgery **74**(1), 246–256.e6 (2021). DOI https://doi.org/10.1016/j.jvs.2020.11.036. URL `https://www.sciencedirect.com/science/article/pii/S0741521420325106`

[4] Chaikof, E.L., Blankensteijn, J.D., Harris, P.L., White, G.H., Zarins, C.K., Bernhard, V.M., Matsumura, J.S., May, J., Veith, F.J., Fillinger,

M.F., et al.: Reporting standards for endovascular aortic aneurysm repair. Journal of vascular surgery **35**(5), 1048–1060 (2002)

[5] Chaikof, E.L., Dalman, R.L., Eskandari, M.K., Jackson, B.M., Lee, W.A., Mansour, M.A., Mastracci, T.M., Mell, M., Murad, M.H., Nguyen, L.L., et al.: The Society for Vascular Surgery practice guidelines on the care of patients with an abdominal aortic aneurysm. Journal of vascular surgery **67**(1), 2–77 (2018)

[6] Demirci, S., Manstad-Hulaas, F., Navab, N.: Quantification of abdominal aortic deformation after evar. In: Medical Imaging 2009: Visualization, Image-Guided Procedures, and Modeling, vol. 7261, p. 72611U. International Society for Optics and Photonics (2009)

[7] Grøndal, N., Bramsen, M., Thomsen, M., Rasmussen, C., Lindholt, J.S.: The cardiac cycle is a major contributor to variability in size measurements of abdominal aortic aneurysms by ultrasound. European Journal of Vascular and Endovascular Surgery **43**(1), 30–33 (2012)

[8] Hoornweg, L., Storm-Versloot, M., Ubbink, D., Koelemay, M., Legemate, D., Balm, R.: Meta analysis on mortality of ruptured abdominal aortic aneurysms. European Journal of Vascular and Endovascular Surgery **35**(5), 558–570 (2008)

[9] López-Linares, K., García, I., García, A., Cortes, C., Piella, G., Macía, I., Noailly, J., Gonzalez Ballester, M.A.: Image-based 3d characterization of abdominal aortic aneurysm deformation after endovascular aneurysm repair. Frontiers in bioengineering and biotechnology **7**, 267 (2019)

[10] Maiora, J., García, G., Macía, I., Legarreta, J.H., Boto, F., Paloc, C., Graña, M., Abuín, J.S.: Thrombus volume change visualization after endovascular abdominal aortic aneurysm repair. In: International Conference on Hybrid Artificial Intelligence Systems, pp. 524–531. Springer (2010)

[11] Stather, P., Sidloff, D., Dattani, N., Choke, E., Bown, M., Sayers, R.: Systematic review and meta-analysis of the early and late outcomes of open and endovascular repair of abdominal aortic aneurysm. Journal of British Surgery **100**(7), 863–872 (2013)

[12] Truijers, M., Fillinger, M.F., Renema, K.W., Marra, S.P., Oostveen, L.J., Kurvers, H.A., SchultzeKool, L.J., Blankensteijn, J.D.: In-vivo imaging of changes in abdominal aortic aneurysm thrombus volume during the cardiac cycle. Journal of Endovascular Therapy **16**(3), 314–319 (2009)